SiliconPV 2024, 14th International Conference on Crystalline Silicon Photovoltaics
Advanced Manufacturing, Challenges for Industrial Devices
https://doi.org/10.52825/siliconpv.v2i.1324
© Authors. This work is licensed under a Creative Commons Attribution 4.0 International License
Published: 03 Jan. 2025

Inline Mapping of Amorphous Silicon Layer Thickness of Heterojunction Precursors Using Multispectral Imaging

Saravana Kumar[1], Christian Diestel[1], Saed Al-Hajjawi[1], Jurriaan Schmitz[2], Marc Hemsendorf[3], Jonas Haunschild[1], Stefan J. Rupitsch[4], and Stefan Rein[1]

[1] Fraunhofer Institute for Solar Energy Systems ISE, Germany

[2] University of Twente, The Netherlands

[3] ISRA VISION GmbH, Germany

[4] University of Freiburg, Germany

*Correspondence: Saravana Kumar, saravana.senthil.kumar@ise.fraunhofer.de

Abstract. In this paper, we present an inline characterization technique to determine spatially resolved thickness maps of ultra-thin layers on textured silicon substrates. The technique is based on multispectral imaging and optical modelling of discrete spectral reflectance data using rigorous polarization ray tracing and the transfer matrix method. The study demonstrates that quantitative inspection of ultra-thin hydrogenated amorphous silicon (a-Si:H) layers on textured silicon substrates requires an extension of the standard RGB illumination by two additional LED wavelengths in the near-UV. As the required five images are measured in less than a second, the tool is a suitable candidate for inline applications. The optical modelling requires reflectance-calibrated images which are obtained via linear calibration functions and allows the a-Si:H thickness to be determined at each pixel. The thin-film thickness can be determined either by a direct modelling of the measured reflectance spectra or by a differential approach using the reflectance spectra before and after coating to eliminate effects from non-idealities due to scattering as well as instrumental errors. The a-Si:H thickness extracted from the reflection data at the five chosen LED wavelengths shows good quantitative agreement with reference values from spectrally-resolved differential reflectance data. Evaluating a test sample with an intentional a-Si:H thickness variation, we compared the results from the multispectral thickness map and reference values from spectroscopic ellipsometry. We found good quantitative agreement for a-Si:H thicknesses above 10 nm and a slight overestimation of about 1.5 nm for thinner layers. Overall, the multispectral approach based on only five different channels proves to allow quantitative thickness maps with reasonable accuracy at inline speed.

Keywords: Amorphous Silicon, Inline Characterization, Silicon Heterojunction Solar Cells, Thickness Maps, Multispectral Imaging

1. Introduction

The market share of silicon heterojunction (SHJ) solar cell technology is expected to rise to 20% in the following decade [1]. A record power conversion efficiency (PCE) beyond 27% has been achieved recently for SHJ solar cells using a back-contact architecture [2]. With increasing PCE, cell performance becomes increasingly sensitive to small defects and inhomogeneities. Their fast detection and avoidance require quick spatially-resolved inline

inspection of the relevant process steps, particularly around the wafer edges, which are prone to inhomogeneities. In an SHJ solar cell, the ultra-thin hydrogenated amorphous silicon (a-Si:H) layers play an important role in providing passivation effects and carrier selectivity. The thickness of these layers ranges from 10 to 20 nm [3]. The performance of an SHJ solar cell is sensitive to the nature of the a-Si:H layers. For instance, a single-nanometer increase in the thickness of a p-doped a-Si:H layer can result in a drop of the short-circuit current density by 0.16 mA/cm^2 [4].

It has been previously demonstrated that the thickness of the ultra-thin a-Si:H layers can be determined with good accuracy from measured inline reflectance data [5], [6]. However, this provides thickness information only along traces with spatial resolution in one dimension. For process control in a production line, full maps of the thin-film thickness across the wafer would be desirable.

In this contribution, we explore the potential of a multispectral tool to determine thickness maps of the ultra-thin a-Si:H layers. Conventionally, the tool is used to determine thickness maps of thicker and colored anti-reflection coating and/or transparent conducting oxide layers via a simple color to thickness calibration without the support of a physical model. Amorphous silicon layers on textured silicon wafers do not change significantly in color in the targeted thickness range. Hence, thickness determination requires physical modeling. First, we identify the optimal wavelengths for measuring reflection to obtain accurate thickness results. Second, we analyze how accurate the thin film thickness can be determined if reflectance values are only available at a small set of spectral supporting points for the optical modeling using the differential approach. Third, the procedure to formulate the calibration functions that helps in translating the greyscale images to reflectance images is described. Finally, evaluating a special test sample with intentional thickness variations, the thickness values from the multispectral approach are compared to reference values from the spectroscopic ellipsometer (SE). In this manner, an optical-model-based thickness mapping procedure using multispectral inline-images is demonstrated for ultra-thin a-Si:H layers.

2. Experimental and theoretical methods

The samples used in this study were made from monocrystalline n-type Cz-Si as-cut wafers (M2 format). The samples were saw-damage-etched followed by alkaline texturing to create random pyramid structures and cleaning with hydrofluoric acid and ozone. The a-Si:H layers were deposited by plasma-enhanced chemical vapor deposition (PECVD). First, a thin intrinsic a-Si:H layer was deposited followed by an n-doped a-Si:H layer. The intrinsic and doped a-Si:H layers are collectively addressed as a-Si:H stack in this contribution. A set of calibration samples with a-Si:H thickness varying between 5-20 nm was prepared by varying the deposition time of both intrinsic and doped a-Si:H layers. Moreover, a special test sample with intentional a-Si:H thickness variation within this wafer was prepared by placing square glass pieces on the sample during deposition. The glass samples are removed sequentially by interrupting the deposition process to create defined a-Si:H thickness variation steps within the wafer.

The characterization tools used in this study are (a) a spectrophotometer (OFR 104 from Zeiss) to record the spectral reflectance with high spectral resolution along a center trace, (b) a spectroscopic ellipsometer (SE) (M-2000 from J. A. Woolam) to measure the effective optical parameters and reference thickness values on planar substrates and (c) a multispectral tool (COL-Q from ISRA VISION GmbH) with modifications in the number of LED wavelengths used in the illumination dome to record the greyscale multispectral images of samples up to M6 format. The multispectral tool is addressed as “prototype COL-Q” tool from here on. It illuminates the wafer sequentially with five sets of LEDs emitting around 640 nm, 520 nm, 470 nm, 420 nm, and 365 nm. The reflectance of the wafer is imaged using an MV4-D1280U-H01-GT camera from Photonfocus. The camera sensor features a quantum efficiency above 30% in the UV-VIS-NIR part of the spectrum. The integration chamber of the tool is coated with

a uniform layer of barium sulphate to create diffuse illumination within the chamber in the whole spectral range. The total recording time for all five greyscale images together is less than a second. The calibration of the spectrophotometer is done with a certified 99% reflective white spectralon standard. The measurement spot diameter of the spectrophotometer is roughly 1 cm with a spectral resolution of 1 nm. The integration time of the spectrophotometer is 24 ms which allows several measurements along the center trace in on-the-fly mode. The spectrophotometer and the prototype COL-Q tool are integrated in a fully automated wafer inspection system from Meyer Burger Technology AG.

An optical model exploiting the transfer-matrix method (TMM) is constructed based on Fresnel equations to simulate the spectral reflectance of thin-films on a textured substrate [6], [7]. The thin-film properties are defined with the help of optical parameters measured using SE. The optical parameters are the refractive index (n) and the extinction coefficient (k) of the thin-film material. The complex refractive index (n + ik) is used to account for refraction and absorption of light in the thin films. It is to be noted that the optical parameters are wavelength-dependent. The effective optical parameters of the a-Si:H stack are used within the optical model and its impact on the estimated thickness values are published elsewhere [5]. The surface geometry of the textured silicon substrate is defined as published by S. Baker-Finch et al. using a fixed pyramid base angle of 54.47° and a variation in pyramid base elevation [7]. Additionally, the model accounts for areas in the wafer with incomplete etching, no pyramids and chemically smoothened pyramids as a planar fraction [8]. The change in polarization of the incident light due to reflection is included with polarization ray tracing matrices as illustrated by Yun et al. [9]. The thickness of the thin-film layer and planar fraction are fitted against the measured reflectance via the Levenberg-Marquardt least-squares fitting algorithm [10]. The thicknesses of ultra-thin layers determined from the direct optical modeling of spectrally-resolved reflectance data are found to deviate from the ground-truth values by a relative error of over 50% [6]. The reason for such errors arises from non-idealities such as a distribution in the pyramid base angles, changes in pyramid geometry and rough pyramid facets present in an actual sample that causes scattering effects [6], [11]. These non-idealities are challenging to be taken into account in the physical model. Furthermore, any calibration error during the measurement of the spectral reflectance can propagate into the fitted thickness. For these reasons, a more reliable approach using differential reflectance to fit the layer thickness of thin-films has been demonstrated earlier [6]. By using the differential approach, the relative error in the fitted thickness decreases by a factor of five as shown in Ref. [6]. A thickness map of a whole wafer is realized by using the developed optical model with the differential approach, and by calibrating the greyscale images from the prototype COL-Q tool to reflectance images, and then fitting for a-Si:H thickness pixel-by-pixel.

3. Results and discussions

3.1 Choice of LED wavelengths in the multispectral tool

Fig. 1 shows the absolute reflectance spectra of the set of textured calibration wafers with intentionally varied a-Si:H stack thickness in the range of 5 to 20 nm. The spectra have been measured with the inline spectrophotometer and are later used to derive calibration functions that convert the measured COL-Q pixel intensities to reflectance. The wavelengths of the LEDs used in the multispectral prototype tool are indicated by the vertical lines in Fig. 1. Concerning the relation between a-Si:H stack thickness and reflectance, Fig. 1 reveals some basic trends: (i) The red channel is rather insensitive to the a-Si:H thickness. (ii) In the green and blue channel, reflectance increases with increasing a-Si:H thickness and its sensitivity being higher for thinner a-Si:H layers. (iii) In the UV channel (at 365 nm), the reflectance signal shows an inverse thickness relation and highest sensitivity of all five channels in the whole thickness range. (iv) The indigo channel (at 420 nm) shows a turnover point between the Green/Blue and the UV channel. Due to the strong thickness sensitivity of the reflectance signal below 550 nm, the a-Si:H layer thickness can be derived from only a few supporting points of the reflectance spectrum. Due to the opposite thickness relation of the reflectance in the UV and the Blue

channel, these two channels are most important for a-Si:H thickness characterization. The red channel, which is less sensitive to a-Si:H thickness variation, may be interesting to identify changes in the textured surface structure. For this reason, the prototype COL-Q tool was equipped with two sets of LEDs with emission peaks around wavelengths 365 nm (Ultraviolet - UV) and 420 nm (Indigo - I) in addition to the standard R-G-B wavelengths. For thickness determination, all five data points (RGB + I + UV) have been used in least-square-fitting to reach highest accuracy. The total number of LED types is limited to five wavelengths due to design constraints of the multispectral system. Moreover, the lowest wavelength is chosen to be 365 nm as below this wavelength the chosen camera loses sensitivity, the required optics become more expensive and the spectra more complex.

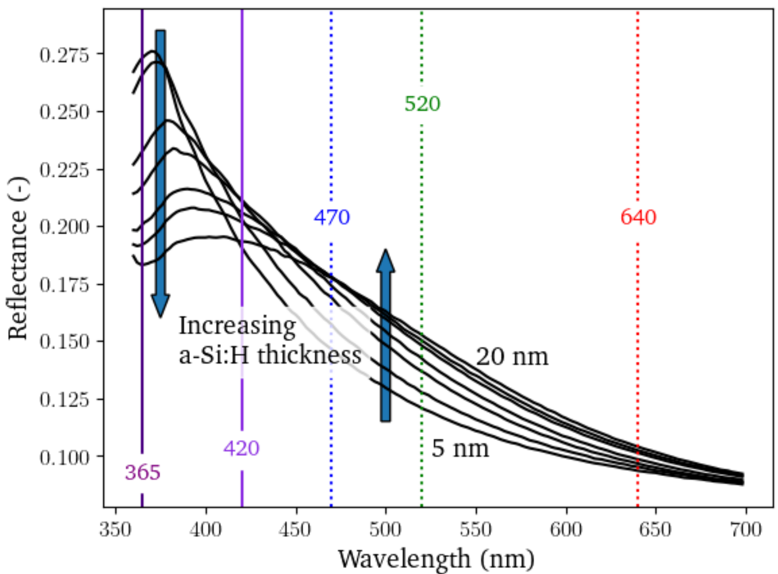

Figure 1. *Spectral reflectance of samples with textured surface and varied a-Si:H stack thickness between 5-20 nm. The LED wavelengths in the standard multispectral tool (640, 520 and 470 nm) are marked with dotted lines and the additional LED wavelengths in the prototype tool (420 and 365 nm) are marked with solid lines.*

3.2 Impact of sparse reflectance data on fit thickness

With the abovementioned theoretical methods, it has been demonstrated that the thickness of thin-films deposited on a textured silicon substrate can be estimated from the absolute reflectance measured on-the-fly in a PV production line [5]. For ultra-thin layers, e.g., a-Si:H layers in an SHJ solar cell, the thicknesses can be predicted with higher accuracies by fitting the so-called differential reflectance spectrum (DRS) rather than the absolute reflectance [6]. The developed optical model becomes robust against nonidealities that differ from theory and instrumental inaccuracies because of the difference-forming nature of the approach [6]. The DRS calculated from the inline reflectance tool has a spectral resolution of 1 nm within the spectral range of 360 to 950 nm. However, using the approach to create thickness maps from the multispectral data allows only 5 data points, from which layer thickness has to be predicted. The impact of using sparse reflection data for thickness determination is studied by fitting the continuous DRS spectrum and the reflection data only at five chosen LED wavelengths using the data measured on a textured sample with 11.6 nm thick a-Si:H stack. The measured differential reflectance data (black symbols) and the corresponding fit curves (red lines) are shown in Fig. 2. The a-Si:H stack thickness determined by using the whole spectral data and by using limited data points are 11 nm (Fig. 2 (a)) and 11.8 nm (Fig. 2 (b)), respectively, which is in close accordance with the reference value of 11.6 nm which has been measured by spectroscopic ellipsometry. This exemplifies the fact that realistic fit thickness can be achieved by just using spare reflectance data at the chosen LED wavelengths and compliments the idea

of realizing thickness maps from multispectral images. Handling fewer data points without the loss of any information makes the prototype COL-Q faster, cheaper and thus inline compatible.

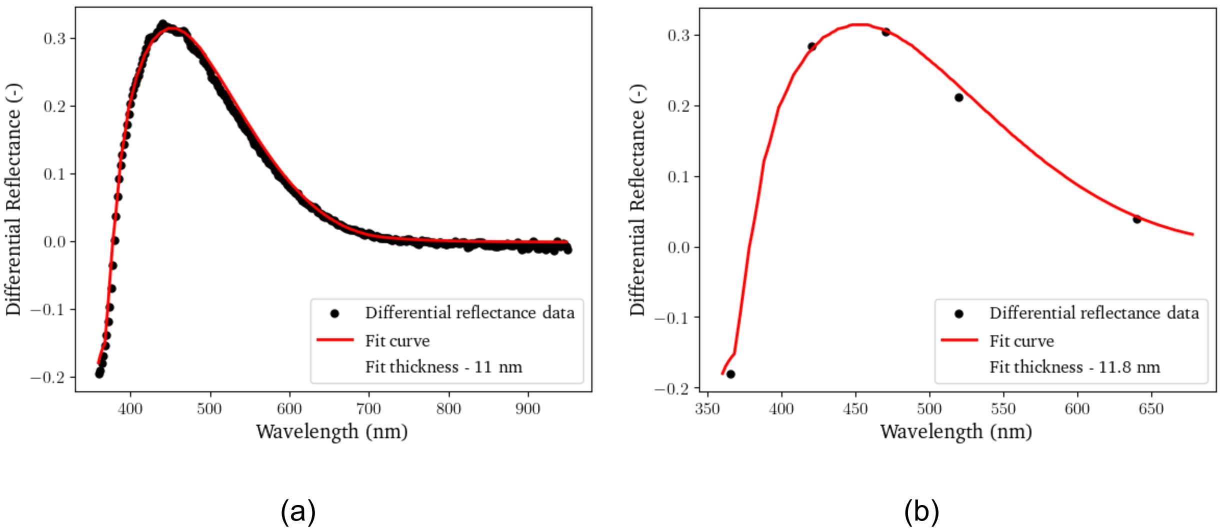

Figure 2. *Differential reflectance data of an a-Si:H stack on a textured silicon substrate (black symbols) and the corresponding fit curve (red solid lines) from the optical model. (a) Fitting the full spectral data, leading to an a-Si:H stack thickness of 11 nm. (b) Fitting only five data points at the chosen LED wavelengths of the prototype multispectral tool, leading to an a-Si:H stack fit thickness of 11.8 nm.*

3.3 Calibrating measured greyscale images to reflectance data

The greyscale images of the special sample with intentional local variation of the a-Si:H stack thickness are shown in Fig. 3. The a-Si:H stack thickness within the sample is varied in steps of 5 nm. It can be clearly seen that the change in pixel intensities due to a-Si:H thickness variations is hardly noticeable in the red channel and clearly seen in the UV channel. Additionally, the patches that appear darker in the green and blue channel appear brighter on the UV channel. This inverse behavior is analogous to the findings from analyzing the reflectance spectra (see Fig. 1).

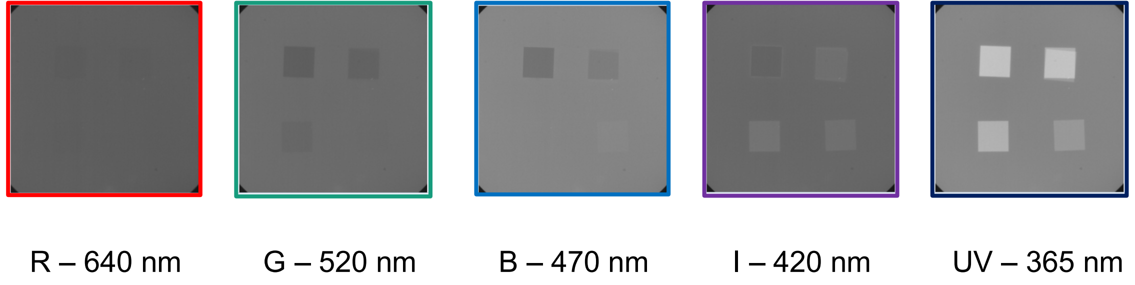

R – 640 nm G – 520 nm B – 470 nm I – 420 nm UV – 365 nm

Figure 3. *Greyscale images from the prototype COL-Q of the special sample with intentional local variation of the a-Si:H thickness. The corresponding LED wavelengths are listed below the images.*

Figure 4 illustrates the normalized emission spectra of the chosen LEDs from the corresponding data sheets. The emission spectra of the LEDs are not strictly monochromatic and different types of LEDs have their unique spectral spread. For instance, the green LED, whose emission spectrum peaks at 520 nm, has a full-width at half-maximum (FWHM) of 35 nm. The spectral spread in the LEDs is taken into account while formulating the calibration functions that convert pixel greyscale intensities to reflectance data. The weights of the

normalized emission intensities across the FWHM of all LEDs are calculated and then used across the reflectance spectra measured from the spectrophotometer. The reflectance values multiplied with their corresponding weights are then added up to arrive at the weighted reflectance values at LED emission peak wavelengths. Thus, the weighted reflectance, *R* can be expressed as

$$R = \sum_{\lambda_i=\lambda_l}^{\lambda_r} r(\lambda_i) w(\lambda_i) \quad (1)$$

where $r(\lambda_i)$ is the reflectance of the sample measured from the spectrophotometer as in Fig. 1, $w(\lambda_i)$ is the weight calculated within the FWHM of the LED emission spectrum as in Fig. 4, and λ_l and λ_r are the wavelengths at the left and right half maximum points around the LED emission peak respectively.

The greyscale images recorded by the multispectral tool have to be calibrated to reflectance values in order to be able to fit the data for thickness values with the optical model. A set of eight different samples with an a-Si:H stack thickness varying between 5 to 20 nm is used in creating the calibration functions. The samples are measured with both the COL-Q prototype and the spectrophotometer. Limited by the measurement spot size of the spectrophotometer, the total weighted reflectance values are correlated to the corresponding modal pixel intensity values within the exact same spot in the full greyscale images. The weighted reflectance is plotted in Fig. 5 as a function of COL-Q median pixel intensities for all the eight calibration samples in all five channels. There exists a linear positive correlation between the spectrophotometer reflectance and the COL-Q pixel intensities in all five channels. The linear fit functions are then used to convert the greyscale images into reflectance-calibrated images. Consequently, each pixel of a combined reflectance-calibrated image will have the absolute reflectance values at the chosen five wavelengths, which is then converted to differential reflectance values using the absolute reflectance data from a reference textured bare silicon sample.

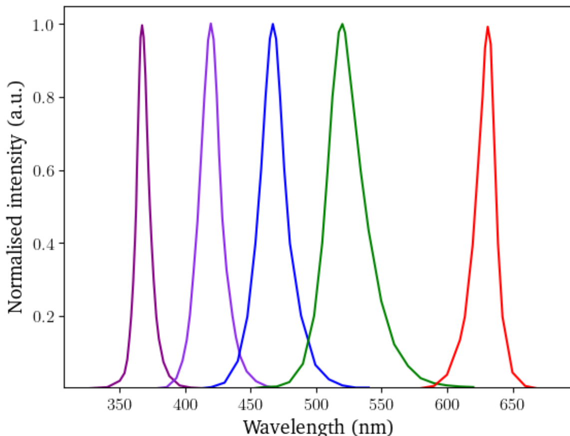

***Figure 4.** Normalized emission spectra from the data sheet of the chosen LEDs in the prototype multispectral tool.*

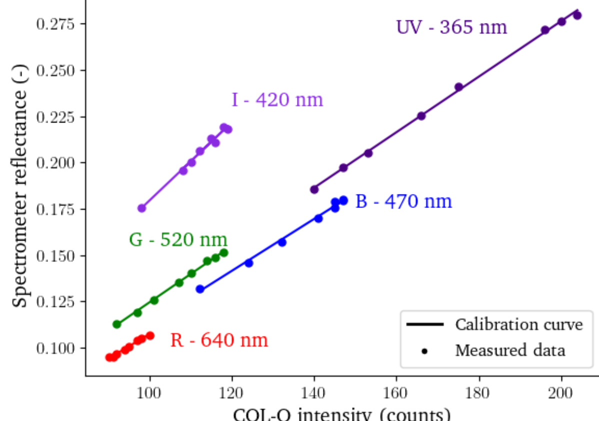

***Figure 5.** Weighted spectral reflectance (from spectrometer) as a function of the modal intensity values in the multispectral images (from COL-Q prototype tool) for the set of calibration sample determined at the exact same spot for the five channels (colored symbols). The corresponding linear fit lines are shown as solid lines.*

3.4 Thickness map

Now that the measured greyscale images from the multispectral tool are transformed to differential reflectance data at each pixel (as in Fig. 2 (b)), the developed optical model can be

finally used to realize the thickness map of the a-Si:H stack on the whole wafer. To reduce the computational time, only the pixels with unique reflectance data set are fitted for thickness with the optical model and stored in a lookup table. The thickness map is then constructed with the help of the lookup table. Using pixel-by-pixel fitting or a lookup table for a single wafer with a million data points could hinder the inline inspection in keeping up with the high throughput rate of a production line. Nonetheless, by using more sophisticated machine learning algorithms, for instance a convolutional neural network, in addition to the optical model, inline compatible processing speed can be achieved [12].

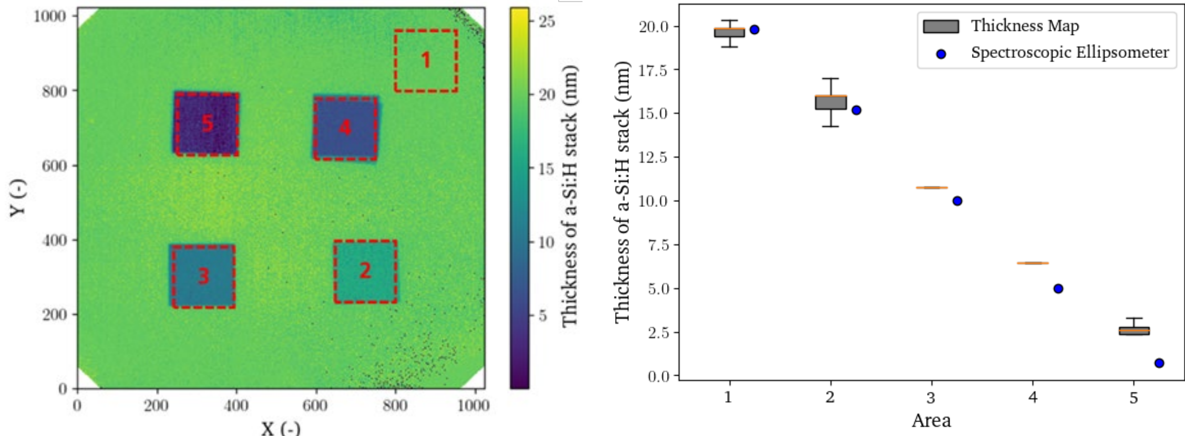

Figure 6. *Thickness map constructed from the recorded multispectral images using the developed optical model with differential approach. Areas in the map numbered and marked in red are analyzed quantitatively in Fig. 7.*

Figure 7. *Fitted thickness values in the marked areas in Fig. 6 (box plots with the median denoted by the orange line) compared to the estimated thickness values from the spectroscopic ellipsometer (blue symbols). The estimated thicknesses are calculated from the glass pieces that were used while making the test sample considering the empirical reduction factor of 1.4.*

Figure 6 shows the a-Si:H stack thickness map of the special test sample determined by the discussed methodology. A few nanometers change in a-Si:H thickness can be clearly seen in the thickness map. A quantitative comparison of the fit thickness in different areas from the multispectral images with respect to the estimated thickness from SE is shown in Fig. 7. The areas from which the fit thicknesses are analyzed are numbered and marked with red squares in Fig. 6. The estimated thicknesses from SE (blue markers) are calculated from the planar glass pieces that were used to block the areas of the test sample from a-Si:H deposition. Additionally, an empirical reduction factor of 1.4 is accounted for the increase in surface area of the textured silicon substrate to arrive at the estimated SE thickness [6], [13]. It should be noted that assuming a fixed reduction factor could lead to a slight discrepancy in the estimated a-Si:H stack thicknesses from SE. However, good agreement between the estimated ellipsometer value and fit values is seen for a-Si:H stack thicknesses above 10 nm. For thicknesses less than 7 nm, there is approximately 1.5 nm absolute difference between the thicknesses from the multispectral fit and from spectral ellipsometry. Moreover, fit thicknesses in certain areas show a dispersion in the a-Si:H thickness values. For instance, a maximum spread of 3 nm is seen in area 2. Such thickness variations could arise from noise in the recorded images but are still comparable to the local a-Si:H thickness variations of roughly 2 nm along the pyramid facets, from pyramid apex to pyramid base, observed earlier from transmission electron microscopy images [6]. We also speculate that the optical parameters (n and k values) in the thinner a-Si:H stack areas deviate from the effective values used in the model. Since the a-Si:H stacks used are a combination of an n-doped a-Si:H layer on an intrinsic a-Si:H layer, the thinner a-Si:H stack areas (areas 4 and 5) could have no or a relatively

thinner layer of n-doped a-Si:H compared to the thicker a-Si:H stack areas. This could also have led to a slight overestimation in the a-Si:H stack fit thicknesses. Additionally, the frequent interruption during the a-Si:H stack deposition to remove the glass pieces could have also affected the optical properties of the thin-film. Camera artefacts that result in unrealistic thickness values appear as black speckles in the thickness maps. This can be eliminated by an improved calibration procedure of the camera. Nevertheless, a-Si:H stack thickness variation across the whole wafer can be perceived from the thickness map obtained from the multispectral images using the optical model.

4. Conclusion

A previously developed optical model is used to fit for thin-film layer thicknesses from measured spectral reflectance from a spectrophotometer or from recorded greyscale images from a multispectral tool. A differential approach is used to reduce the discrepancies in fit thicknesses that arise from instrumental inaccuracies and optical non-idealities that are difficult to incorporate in the optical model. Using the model to fit for thicknesses from the whole spectral reflectance and from using only five data points leads to similar fit thicknesses, which is promising to use multispectral image data for constructing thickness maps. The images recording time of the multispectral tool being less than a second makes it compatible for inline characterization applications. To characterize ultra-thin a-Si:H stacks, as in an industrial SHJ solar cell, it is beneficial to have greyscale images in the near-UV part of the spectrum in addition to the standard RGB images. A linear positive correlation between reflectance and the multispectral image intensities is observed in all the chosen wavelengths. The linear calibration functions convert the multispectral images to reflectance calibrated images, which are then fed into the optical model to fit for layer thicknesses via the differential approach. The proof of concept is illustrated on a special sample with intentional variation of the a-Si:H stack thickness. For thicknesses above 10 nm, a good agreement between the estimated thickness from SE and the fitted thickness is seen. For lower thicknesses, only a slight absolute difference of around 1.5 nm is seen. This could have arisen from slight discrepancies in the optical parameters in the areas with thinner a-Si:H stacks. Unrealistic thickness values arriving from camera artefacts could be eliminated by a proper calibration of the camera. Nevertheless, a fast inline-compatible method to realize thickness mapping of ultra-thin a-Si:H layers in SHJ solar cells from multispectral images is successfully demonstrated.

Data availability statement

The relevant data and the code used within this contribution are confidential.

Underlying and related materials

The reflectance of thin-films on a substrate is calculated from the python software package – “tmm” created by Steven J. Byrnes. Available online - https://arxiv.org/abs/1603.02720v5

Author contributions

Saravana Kumar performed writing – original draft, conceptualization, methodology and validation. Christian Diestel and Saed Al-Hajjawi performed conceptualization and methodology. Marc Hemsendorf provided the resources. Stefan J. Rupitsch supported with supervision. Jurriaan Schmitz performed supervision, writing – review & Editing, formal analysis and validation. Jonas Haunschild and Stefan Rein performed supervision, writing – review & Editing, project administration and funding acquisition.

Competing interests

The authors declare that they have no competing interests.

Funding

This work has been funded by the German Federal Ministry for Economic Affairs and Climate Action within the project SALSA under contract number 03EE1096A.

Acknowledgement

The authors thank Ioan Voicu Vulcanean for preparing the samples and Jonas Schönauer for supporting with image processing.

References

[1] ITRPV report from VDMA, 15th edition, Mar., 2024.
[2] LONGi news, [Online]. Available: https://www.longi.com/en/news/heterojunction-back-contact-battery/
[3] P. Procel, H. Xu, A. Saez, C. Ruiz-Tobon, L. Mazzarella, Y. Zhao, C. Han, G. Yang, M. Zeman, and O. Isabella, “The role of heterointerfaces and subgap energy states on transport mechanisms in silicon heterojunction solar cells”, Prog. Photovolt., Res. Appl., vol. 28, no. 9, pp. 935–945, May, 2020, doi: 10.1002/pip.3300.
[4] Z. C. Holman, A. Descoeudres, L. Barraud, F. Zicarelli Fernangez, J. P. Seif, S. de Wolf, and C. Ballif, “Current Losses at the Front of Silicon Heterojunction Solar Cells”,IEEE Journal of Photovoltaics 2, pp. 7-15, Jan., 2012, doi: 10.1109/JPHOTOV.2011.2174967.
[5] S. Kumar, H. Vahlman, S. Pingel, I. Voicu Vulcanean, A. Steinmetz, J. Haunschild, S. J. Rupitsch, and S. Rein, “Characterization of thin-film structures of silicon heterojunction solar cells with inline reflectance spectroscopy”, AIP Conf. Proc., vol. 2826, Art. no. 030005, June, 2023, doi: 10.1063/5.0141006.
[6] S. Kumar, H. Vahlman, S. Al-Hajjawi, C. Diestel, J. Haunschild, S. J. Rupitsch, and S. Rein, “Inline characterization of Ultrathin Amorphous Silicon Stacks in Silicon Heterojunction Solar Cell Precursors with Differential Reflectance Spectroscopy”, IEEE Journal of Photovoltaics 13, pp. 711-715, July, 2023, doi: 10.1109/JPHOTOV.2023.3301132.
[7] S. C. Baker-Finch and K. R. McIntosh, “Reflectance of normally incident light from silicon solar cells with pyramidal textures”, Prog. Photovolt: Res. Appl. 19, pp. 406-416, June, 2011, doi: 10.1002/pip.1050.
[8] K. Birmann, M. Demant, and S. Rein, “Optical characterization of random pyramid texturization”, Proc. Eur. PV Sol. Energy Conf. Exhib., Hamburg, Germany, pp. 1454–1458, Sept., 2011, doi: 10.4229/26thEUPVSEC2011-2BV.2.181.
[9] G. Yun, K. Crabtree, and R. A. Chipman, “Properties of the polarization ray tracing matrix”,Proc. SPIE, Art. no. 66820Z, vol. 6682, September, 2007, doi: 10.1117/12.734315.
[10] S. J. Rupitsch, “Characterization of sensor and actuator materials,” in Piezoelectric Sensors and Actuators: Fundamentals and Applications, (Springer, Berlin, July, 2018), pp. 143–144.
[11] S. C. Baker-Finch and K. R. McIntosh, “Reflection distributions of textured monocrystalline silicon:implications for silicon solar cells”, Prog. Photovolt: Res. Appl. 21, pp. 960-971, Mar., 2012, doi: 10.1002/pip.2186.
[12] O. Ronneberger, P. Fischer, and T. Brox, “U-Net: Convolutional Networks for Biomedical Image Segmentation”, MICCAI, Springer, Cham. pp. 234-241, May, 2015, doi: 10.48550/arXiv.1505.04597.
[13] D. Pysch, M. Bivour, M. Hermle, and S. Glunz, “Amorphous silicon carbide heterojunction solar cells on p-type substrates”, Thin Solid Films, vol. 519, pp. 2550–2554, Feb., 2011, doi: 10.1016/j.tsf.2010.12.028.